Carbohydrate Polymer Technologies and Applications 2 (2021) 100130

Contents lists available at ScienceDirect

Carbohydrate Polymer Technologies and Applications

journal homepage: www.sciencedirect.com/journal/carbohydrate-polymer-technologies-and-applications

Effect of charge balancing cations on the viscoelastic and thermal properties of welan

Chengrong Wen [a,b], Zhongqi Sun [b], Mohamed Salem Elfaruk [c,d], Anjaneyulu Putta [e], Jie Pang [b,*], Srinivas Janaswamy [c,*]

[a] Collaborative Innovation Center of Seafood Deep Processing, National Engineering Research Center of Seafood, National & Local Joint Engineering Laboratory for Marine Bioactive Polysaccharide Development and Application, School of Food Science and Technology, Dalian Polytechnic University, Dalian, 116034, China
[b] College of Food Science, Fujian Agriculture and Forestry University, Fuzhou, Fujian 350002, PR China
[c] Department of Dairy and Food Science, South Dakota State University, Brookings, SD 57007, USA
[d] Medical Technology College, Nalut University, Nalut 00218, Libya
[e] Department of Chemistry Center for Fluorinated Functional Materials, University of South Dakota, Vermillion, SD, 57069, USA

ARTICLE INFO

Keywords:
Welan
Divalent cation
Rheology
Thermal properties

ABSTRACT

Welan is a branched polymer in the gellan family of polysaccharides. It has good compatibility with divalent calcium ions with a potential use in cementing applications. It is also been utilized as an anti-washout material for underwater concrete placement. Herein, influence of divalent cations Ca^{2+}, Ni^{2+}, Mg^{2+}, Zn^{2+} and Sr^{2+} on the gelling and thermal properties of welan have been investigated. The viscoelastic properties reveal strong gelation behavior that are stable up to 80 °C. Among all the five cations Ni^{2+}, Ca^{2+}, Zn^{2+} and Sr^{2+} are suited well, compared to Mg^{2+} ions, to promote favorable interactions among the welan chains leading to stronger junction zones and elastic moduli. The melting peak and enthalpy are dependent on the nature and size of the divalent cation. The outcome is deemed to aid to expand the welan utility in food and non-food applications.

1. Introduction

Gellan family polysaccharides namely gellan, welan, rhamsan and S657 are a group of anionic bacterial exopolysaccharides that are economically competitive compared to plant and seaweed polysaccharides - (Edwin, Katsuyoshi,& Marguerite, 2012). Due to their intrinsic natural origin, plant and seaweed polysaccharides could get influenced by the environmental factors leading to variable molecular chains and weights that in-turn influence the physicochemical properties. On the other hand, bacterial polysaccharides produced by microorganisms under controlled environmental conditions result in rather robust and unique structures. Consequently, bacterial polysaccharides have gained attention in food and pharmaceutical applications and their versatile solution and gelation properties are quite handy to develop a variety of functional products. Among the bacterial polysaccharides, welan, also known as S-130, is a heteropolysaccharide (Fig. 1) with a high molecular weight of 1.0×10^6 g/mol. It's main chain is composed of a tetrasaccharide repeat of β-1,3-D-glucopyranose, β-1,4-D-glucuronopyranose, β-1,4-D-glucopyranose and α-1,4-L-hamnopyranose along with a side group of L-rhamnopyranose or L-mannopyranose substituted at the O-3 atom in the 4-linked glucopyranosyl unit in an approximate ratio of 2:1. In addition, one O-acetyl group per two repeating units along with acetyl and glyceryl groups at the O-2 and O-6 atoms on the β-1,3-D-glucopyranose (Sakata et al., 2001; Diltz & Zeller, 2001; Rinaudo, 2004; Tako et al., 2009; Kaur et al., 2014) are also noticed.

The side chains significantly influence solution properties among the gellan family polysaccharides. For example, gellan forms strong thermal reversible gels but welan does not gel either in the native or deacetylated form, instead yields high viscous solutions with good thermal stability (Crescenzi, & Dentini, 1987; Sandford, Cottrell, & Pettitt, 1984). Welan is primarily marketed for its excellent stability over a wide pH range (Crescenzi, & Dentini, 1987; Rols, Ambroise, & Péra, 1999; Hoskin, Mitchell, & Shu, 1991; Plank, 2004). It's thickening, suspending and stabilizing properties, indeed, gained great commercial potential especially in food, concrete, petroleum extraction and ink processing (Mohammed, 2006; Plank, Lummer & Dugonjic-Bilic, 2010; Sonebi, 2006; Sonebi, & Malinov, 2011) applications, to name a few.

Like the other members of the gellan family, welan also prefers a double helical molecular structure despite the presence of a side group and substituents Chandrasekaran, Radha & Lee (1994). The helix is

* Corresponding authors.
E-mail addresses: pang3721941@163.com (J. Pang), Srinivas.Janaswamy@sdstate.edu (S. Janaswamy).

https://doi.org/10.1016/j.carpta.2021.100130
Received 27 November 2020; Received in revised form 12 July 2021; Accepted 30 July 2021
Available online 31 July 2021

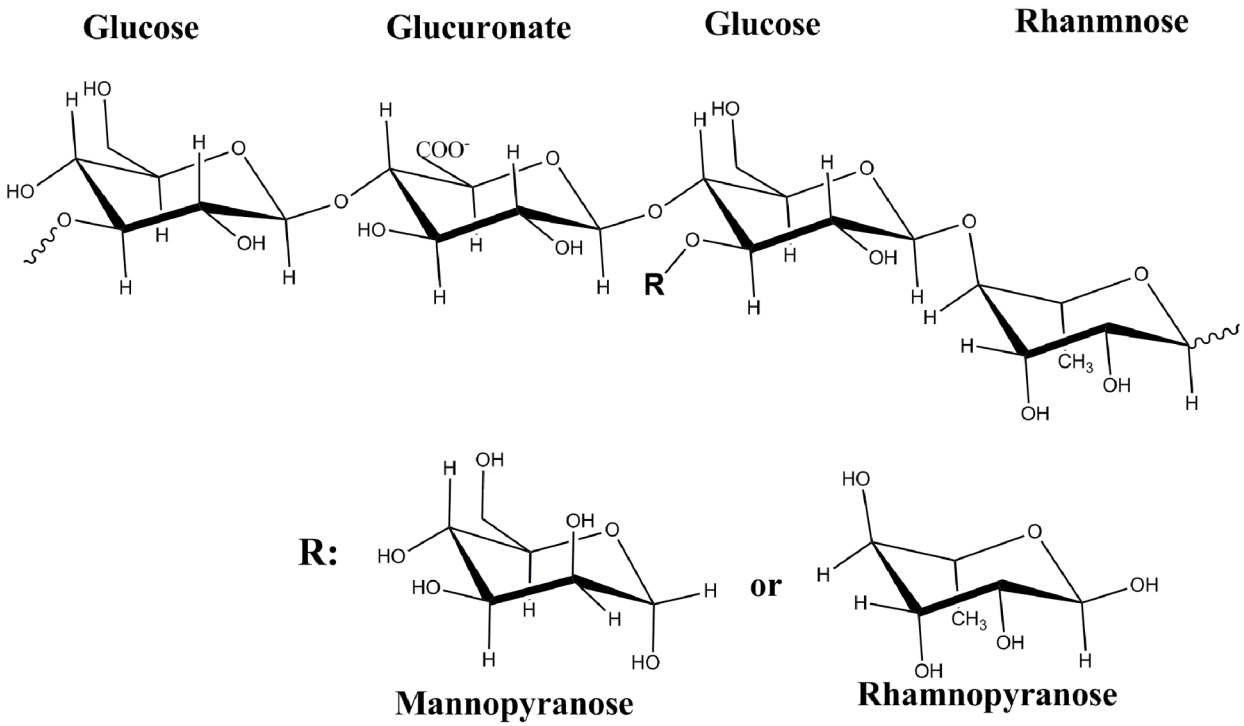

Fig. 1. Chemical structure of welan.

stabilized by a series of hydrogen bonds between the carboxylate groups and the side chain, and the inter-helical associations are promoted through strong carboxylate-cation-carboxylate interactions. Toward this end, calcium ions are found to be suitable to orchestrate stable packing structure. However, there are no systematic reports on welan's structure-property relationships in the presence of divalent ions. We hypothesis that size and nature of cation influence the functional properties of welan, and the present study is aimed at understanding the influence of five selected divalent cations Ca^{2+}, Ni^{2+}, Mg^{2+}, Zn^{2+} and Sr^{2+} on the solution and thermal properties of welan.

2. Experimental

2.1. Materials

Welan was a gift from CP Kelco, USA. The analytical grade $CaCl_2$, $NiCl_2 \bullet 6H_2O$, $MgCl_2 \bullet 6H_2O$, $ZnCl_2$, and $SrCl_2 \bullet 6H_2O$ were purchased from VWR, Mallinckrodt, Fisher Scientific and Sigma-Aldrich. Reagent grade isopropyl alcohol and distilled deionized water (DDW) were used as necessary.

2.2. Preparation of divalent welan (DW)

The amount of 200 mg welan was dispersed in 200 mL DDW with constant magnetic stirring and heated to and held at 95 °C for 1 h. Subsequently, 100 mM of salt was added and the solution was further heated for 1 h with continuous stirring. The total solution volume was maintained at around 200 mL by adding required quantity of DDW, as and when necessary. The hot solution was then poured into 400 mL of cold isopropyl alcohol (~0 °C). The precipitate was collected and was washed twice with 80% w/w, and later with 100% isopropyl alcohol. The final product was dried at 55–60 °C for 24 h. From each of the salt form, two concentrations of 0.5 and 1.0% w/w homogeneous solutions were prepared by dispersing 5 and 10 mg/mL, respectively, in DDW. The Mg, Ca, Ni, Zn and Sr salt forms have been referred as WMg, WCa, WNi, WZn and WSr, respectively, for brevity, in the rest of the discussion.

2.3. Fourier transform infrared (FTIR) and nuclear magnetic resonance (NMR) spectroscopy

The FTIR spectra were collected using the Spectrum 100 FT-IR from PerkinElmer, USA spectrophotometer. The data were recorded at room temperature in the wave number range 380–4000 cm^{-1}, and a total of 4 scans at a resolution of 4 cm^{-1} were co-added for each spectrum.

The NMR spectral studies were carried out using D_2O as solvent at room temperature (25 °C) on Bruker Avance III HD 400 MHz NMR spectrometer. For all compounds, 1% solution was used and average spectrum from 16 scans are reported. The chemical shifts are expressed in parts per million (ppm).

2.4. Solution properties

The viscoelastic measurements were performed using cone and plate geometry (40 mm diameter; 0.05 rad cone angle) on the ARG2 mechanical spectrometer from the TA Instruments, New Castle, DE. Linear viscoelastic region was identified from the strain sweep measurements in the range 0.01% to 20% strain at 1Hz and 5 °C. The storage modulus (G') and loss modulus (G″) were measured at 1% strain (in the linear viscoelastic range) (a) in the frequency range 0.1 to 100 Hz at three selected temperatures: 5, 25 and 45 °C, and (b) in the temperature range 5 to 80 °C with a heating rate of 2 °C/min at 1Hz. Average values from duplicate experiments are reported.

2.5. Melting properties

Modulated Differential Scanning Calorimetry (mDSC) was carried out using the DSC Q2000 from the TA Instruments, New Castle, DE. The equipment was calibrated with an indium disk. The samples were equilibrated at 75% RH for 2 days, and 2.5 ± 0.1 mg were sealed in the Tzero aluminum hermetic pan and analyzed under a nitrogen gas flow of 50 mL/min. A modulation of ±0.68 °C/min was used and the temperature was ramped from 40 to 230 °C at a constant rate of 5°C/min. The Universal Analysis 2000 software (TA Instruments, New Castle, DE) was

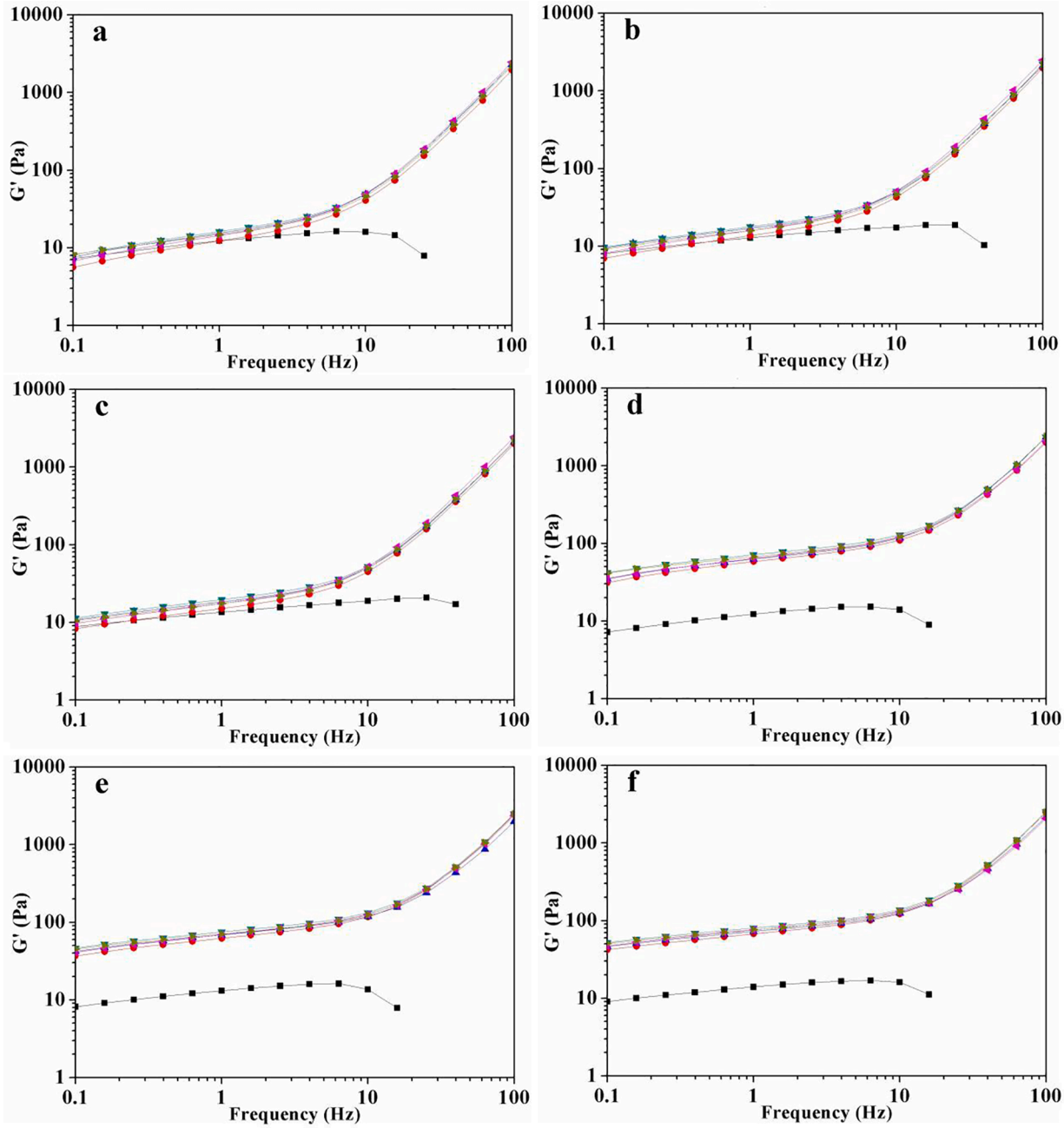

Fig. 2. Variation in the viscous moduli (G') for the 0.5% welan solutions as a function of frequency at (a) 45, (b) 25 and (c) 5 °C, and for the 1.0% solutions at (d) 45, (e) 25, and (f) 5 °C. Black squares, red circles, blue up triangles, dark cyan down triangles, magenta left Tries and dark yellow right Tries correspond to commercial welan, WMg, WCa, WNi, WSr and WZn, respectively.

used to estimate the peak temperature and enthalpy of melting endotherm. Samples were tested in duplicate and average values are reported.

3. Results and discussion

3.1. Viscoelastic properties of solutions - Frequency dependence

In all the solutions, the elastic moduli (G') is far greater than the loss moduli (G″) in the frequency range 0.1–100 Hz portraying a typical gel-like behavior by welan (Fig. 2 a-f). The cation type and size appear to have a subtle influence. The elastic moduli (G') for the 0.5% solutions, at 1 Hz and 5 °C, are 18, 17, 15, 10 and 9 Pa for WNi, WCa, WZn, WSr and WMg, respectively. At higher frequencies, substantial increase in the G' is noticed, for example, around 3000 Pa at 100 Hz suggesting the temporary association among the welan chains during the short oscillation periods. More or less, similar values are observed at 25 and 45 °C too attesting the stable nature of the welan solutions. At the higher polysaccharide concentration of 1.0% similar trend in the G' is observed except that the individual values are 4 orders more than that of the 0.5% concentration.

Generally tan(δ) $\left(=\frac{G''}{G'}\right)$ provides a good evaluation criterion for assessing the sol-to-gel transition of polysaccharide solutions. When tan

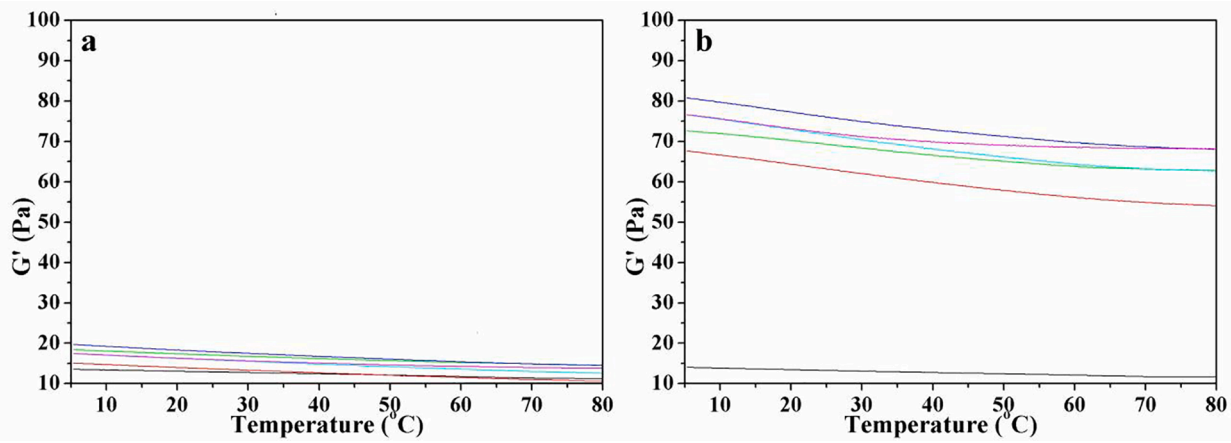

Fig. 3. Variation in the viscoelastic properties G' (solid) as a function of temperature of (a) 0.5% w/w and (b) 1.0% w/w at 1% w/w strain (linear region), 1Hz frequency. black squares are commercial welan, red circles WMg, Blue up triangles WCa, dark cyan down triangles WNi, magenta left Tries WSr^{+}, dark yellow right Tries WZn.

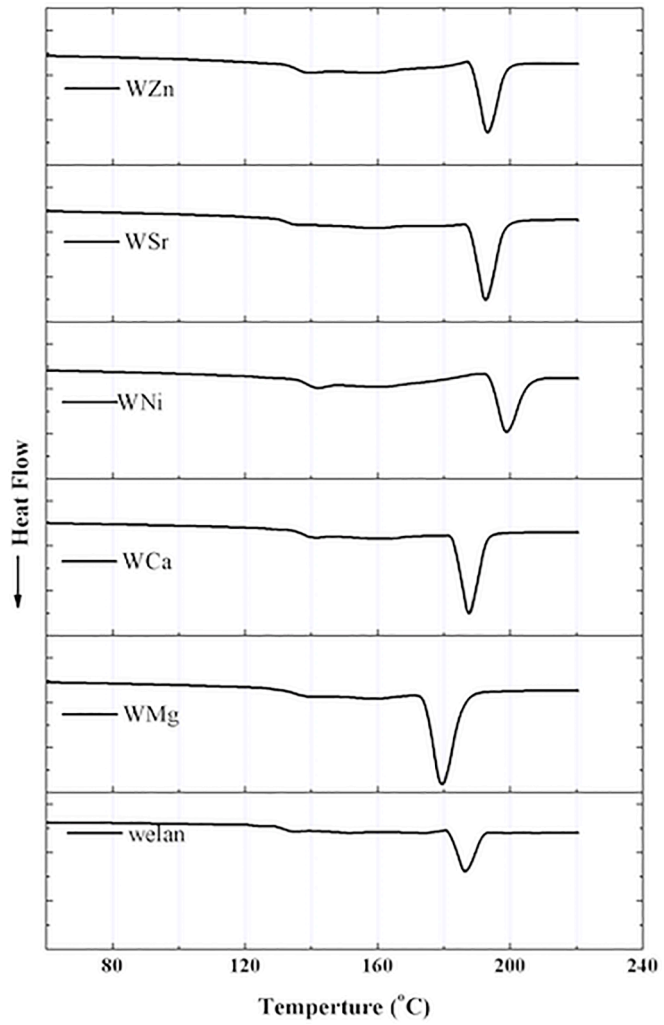

Fig. 4. Variation in mDSC of welan and DW from 40 °C to 230 °C.

(δ) is >1, the solution possesses liquid-like behavior, while <1 suggests the solid-like and elastic characteristics. Herein, tan(δ) values of DW are slightly higher than that of commercial welan at 0.5% w/w at low frequencies (Fig S1, supplementary material). In addition, they decrease with the frequency increase, while those of divalent form are well stabilized. Overall, it appears that in the low frequency region, 0.1–3 Hz, influence of divalent cations is quite subtle but at higher frequencies cations stabilize the gel network significantly, consistent with increased elastic moduli.

3.2. Viscoelastic properties of solutions - Temperature dependence

In the temperature range 5 to 80 °C, the 0.5 and 1.0% solutions display typical gel-like behavior with elastic moduli (G') far greater than the loss moduli (G″) (Fig. 3a &3b). As noticed in the frequency sweep measurements, even in the temperature ramp, cations did not exhibit significant differences. The observed G' values are 19.2, 18.1, 17.1, 17.0, and 14.7 Pa for WNi, WCa, WZn, WSr and WMg, respectively. The tan(δ) values reveal minimal dependence and the solutions are in gel state even at 80 °C (Fig. S2). Among all the five divalent cations employed in this study, it appears that Ni^{2+}, Ca^{2+}, Zn^{2+} and Sr^{2+} ions are suited well, compared to Mg^{2+} ions, to promote favorable interactions among the welan chains leading to stronger junction zones and elastic moduli.

3.3. Melting behavior of solutions

Fig. 4 depicts the total heat signal from the mDSC analysis. The melting endotherm of pure welan was around 190 °C; however, presence of divalent cations brings out appreciable change. The WNi, WCa, WZn, WSr and WMg display endothermic peak at 199, 187, 193, 192 and 180 °C, respectively, and the larger spread certainly indicates the preferential role of cations in promoting favorable interactions among the welan chains. The observed 19 °C higher peak temperature of WNi as compared to WMg further suggests that Ni^{2+} ions are more suited for stabilizing the welan chains than the Mg^{2+} ions. These results are in accord with the viscoelastic properties wherein increased elastic moduli (G') is noticed in the presence of Ni^{2+} ions than the Mg^{2+} ions. Surprisingly, the melting enthalpies (△H) do not follow this trend. The △H of WNi, WCa, WZn, WSr and WMg is 104.8, 119.9, 115.5, 125.5 and 117.2 J/g, respectively. The differences could be presumably due to the number of welan helices involved in the junction zone formation as well as the number of junction zones. The △H of commercial welan is around 80.5 J/g, far less than that of the divalent forms suggesting the preferential role of divalent ions toward modulating the welan thermal behavior.

3.4. Spectroscopic analysis

In order to further understand the role of cations, commercial welan

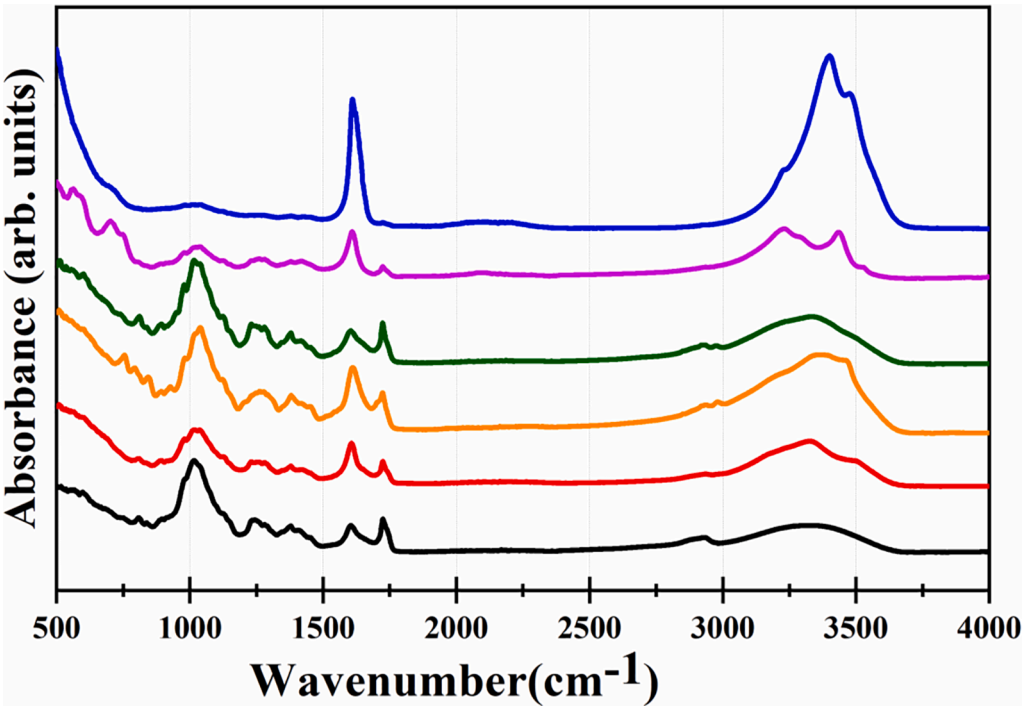

Fig. 5. Comparison of FTIR spectra of commercial welan, WMg, WZn, WNi, WSr and WCa, from bottom to top, in the spectral region of 500 to 4000 cm^{-1}.

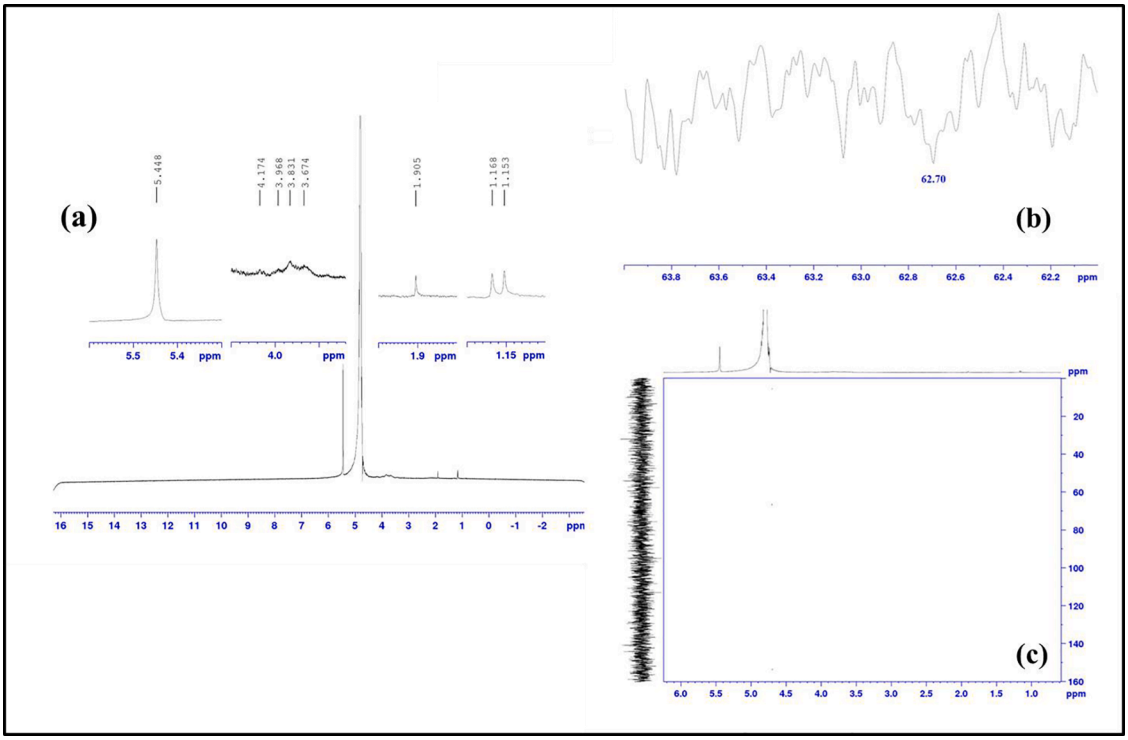

Fig. 6. The NMR spectra of calcium welan in D_2O. (a) ^1H, (b) DEPT and (c) HSQC spectrum.

and welan complexes WCa, WZn, WNi, WSr and WMg are analyzed through FTIR and the corresponding spectra are shown in Fig. 5. In the case of commercial welan the band at 3334 cm^{-1} is due to –OH stretching. It is intact in the prepared complexes; however, with the presence of divalent cations on the welan backbone additional three distinct peaks at 3221, 3393 and 3475 cm^{-1} are observed. More interestingly, their intensity increases leading to sharper speaks with the presence of Sr^{2+}, Zn^{2+} and Ca^{2+} ions. These changes could be due to the formation of new ionic bonds between OH groups and cations. The band at 2895 cm^{-1} indicates the stretching vibration of the -CH_2 groups. Its intensity reduces with the addition of Ca^{2+} and Sr^{2+} ions and shifts to 2944 cm^{-1} with Mg^{2+} ions. Surprisingly, it splits into peaks 2908, and 2983, and 2946 and 2987 cm^{-1} in WNi and WZn, respectively. These changes clearly accentuate the bonding of divalent ions on to the welan and their synergistic effect. The C-O-C and C-O-H tensile vibrations are observed at 1234 cm^{-1} and 1026 cm^{-1}, respectively. The strong band at

around 1069 cm^{-1} was attributed to the C-O-C stretching. The peaks in the range 1380–1730 cm^{-1} represent the symmetrical and unsymmetrical COO^- group stretching vibrations. In the present case the bands at 1610 cm^{-1} and 1365 cm^{-1} are attributed to COO- asymmetric and symmetrical vibration.

The ^1H NMR spectrum of calcium welan (WCa) is shown in Fig. 6a. The characteristic proton signals at δ 5.45 and 4.17 ppm corresponds to α L-mannosyl and α L-rhamnosyl residues and β-D-glucuronosyl and β-D-glucosyl residues, respectively. The methyl protons (H-6) of two rhamnose residues are observed as a doublet at δ 1.17 and 1.15 ppm. The singlet at δ 1.91 ppm indicates acetylated monosaccharide corresponding to acetyl groups at O(6) of the 3-linked glucose residue in the tetrasaccharide repeat unit. Similar spectra is noticed with other cations and control welan samples as well. The ^{13}C DEPT and 135 NMR spectrum (Fig. 6b) displays a feeble negative ^{13}C NMR signal at around δ 62-63 ppm due to CH_2OH group related to the C-6 non-substituted mannose residues. The HSQC spectrum (Fig. 6c) is not quite informative suggesting that 1% w/w solution used in this study might not be adequate. However, at higher concentrations, formation of thick gels precludes further NMR analysis. Similar observations are noticed for WZn, WNi, WSr and WMg and commercial welan as well. Thus, it appears that high molecular weight, high viscosity and gel forming polysaccharides might not be amenable for NMR analysis toward gaining meaningful structural information.

In the gellan family, carboxylate-carboxylate interactions mediated by cations and water molecules play significant role on the junction zone architecture and in-turn on the solution and thermal properties. The three-dimensional structure analysis reveals that in the smallest possible junction zone arrangement of gellan there are two double helices that associate through $COO^-\bullet\bullet\bullet K^+\bullet\bullet\bullet W\bullet\bullet\bullet K^+\bullet\bullet\bullet COO^-$ interactions, wherein COO^-, K^+, and *W* represent carboxylate group, potassium ion and water molecule, respectively (Chandrasekaran et al, 1988). However, replacement of K^+ with Ca^{2+} ions leads to molecular aggregates due to random crosslinking as the COO^- groups are on the helix periphery. On the other hand, in the case of welan more organized networks could be obtained in the presence of divalent Ca^{2+} ions, as the side group folds back on to the helix and partially shield the COO^- groups from the surroundings. In the smallest possible junction zone three welan double helices interact via a series of $COO^-\bullet\bullet\bullet Ca^{2+}\bullet\bullet\bullet COO^-$ and $COO^-\bullet\bullet\bullet W\bullet\bullet\bullet Ca^{2+}\bullet\bullet\bullet COO^-$ interactions (Chandrasekaran, Radha & Lee, 1994). The divalent cations induced direct interactions among the adjacent welan helices would indeed reflect on the viscoelastic and thermal properties. However, for a variety of divalent ions the relative strengths of these interactions could alter leading to changes in the overall macroscopic behavior. The Shannon ionic radii for Ni^{2+}, Ca^{2+}, Zn^{2+}, Sr^{2+} and Mg^{2+} are 0.69, 1.06, 0.74, 1.18 and 0.72 Å, respectively Shannon (1976). The coordination of these cations is 6, 7, 6, 6 and 6, in the same order. Hence, depending on the divalent cation type and its coordination number the relative strengths of $COO^-\bullet\bullet\bullet M^{2+}\bullet\bullet\bullet COO^-$ and $COO^-\bullet\bullet\bullet W\bullet\bullet\bullet M^{2+}\bullet\bullet\bullet COO^-$, wherein M represent the divalent cation, interactions would vary, which in turn will influence the inter-helical spacing among the neighboring welan helices and impact the overall network strength. All these changes occurring at the molecular level appear to be responsible for the observed macro level variations in the viscoelastic and thermal properties. Further research is needed to gain more knowledge on the junction zone architecture and subsequent effect on the structure-function relationships of welan.

4. Conclusions

The solution properties of polysaccharides depend largely on their intrinsic physicochemical characteristics such as molecular weight, polydispersity and degree of substitution as well as their molecular shapes and interactions with the surrounding cations and water molecules. Herein, influence of divalent cations on the viscoelastic properties and thermal behavior as well as FTIR and NMR spectra of welan has been studied. The results suggest that divalent cations are suited well to improve solution and thermal properties of welan. More experimental data, especially in the presence of monovalent cations, however, is needed to further decipher the structure-function relationships of welan and expand its utility beyond non-food applications. Indeed, variations in the macroscopic behavior of welan could stem from the alterations in the three-dimensional network composed of double helical junction zones. In this regard, knowledge about the exact location of cations and their roles in modifying the molecular structure would shed light on expanding the commercial potential and industrial usage of this important bacterial polysaccharide. The outcome could further serve as a new tool for current and next-generation applications of welan *e.g.* carries of bioactive compounds (Janaswamy & Youngren, 2012; Janaswamy et al., 2013; Polowsky & Janaswamy, 2015), films (Larotonda et al., 2015; Wu et al., 2019), protein-polysaccharide mixtures (Yan et al., 2019), fibers (Dong et al., 2020), beads (Nie et al., 2021) and hydrogels (Yu et al., 2015), to name a few, leading to novel welan-based food supplements, functional foods and medicinal foods, though, so far, welan has mostly been exploited for non-food applications (Tenga, Meng & Khayata, 2020).

Declaration of Competing Interest

Authors declare no conflict of interest.

Acknowledgements

Research was supported by the College of Food Science Fujian Agriculture and Forestry University, foundation projects of National Natural Science Foundation of China (31271837 and 31471704), USDA National Institute for Food and Agriculture (SD00H648-18) and the Libyan Scholarship Program PhD grant (08/2014).

Supplementary materials

Supplementary material associated with this article can be found, in the online version, at doi:10.1016/j.carpta.2021.100130.

References

Chandrasekaran, R., Puigjaner, L. C., Joyce, K. L., & Arnott, S. (1988). Cation interactions in gellan: An X-ray study of the potassium salt. *Carbohydrate Research, 181*, 23–40.
Chandrasekaran, R., Radha, A., & Lee, E. J. (1994). Structural Roles of calcium-ions and side-chains in welan - An X-ray study. *Carbohydrate Research, 252*, 183–207.
Crescenzi, V., & Dentini, M. (1987). The influence of side-chains on the dilute-solution properties of three structurally related, bacterial anionic polysaccharides. *Carbohydrate Research, 160*, 283–302.
Diltz, S., & Zeller, S. G. (2001). Location of O-acetyl groups in S-657 using the reductive-cleavage method. *Carbohydrate Research, 331*, 265–270.
Dong, M., Zhang, K., Wang, L., Han, J., Wang, Y., Xue, Z., & Xia, Y. (2020). High-strength carrageenan fibers with compactly packed chain structure induced by combination of Ba^{2+} and ethanol. *Carbohydrate Polymers, 236*, Article 116057.
Edwin, R. M., Katsuyoshi, N., & Marguerite, R. (2012). Gelation of gellan - A review. *Food Hydrocolloids, 28*, 373–411.
Hoskin, D. H., Mitchell, T. O., & Shu, P. (1991). *U.S. Patent No. 4,991,652*. Washington, DC: U.S. Patent and Trademark Office.
Janaswamy, S., & Youngren, S. R. (2012). Hydrocolloid-based nutraceutical delivery systems. *Food & Function, 3*, 503–507.
Janaswamy, S., Gill, K. L., Campanella, O. H., & Pinal, R. (2013). Organized polysaccharide fibers as stable drug carriers. *Carbohydrate Polymers, 94*, 209–215.
Kaur, V., Bera, M. B., Panesar, P. S., Kumar, H., & Kennedy, J. F. (2014). Welan gum: Microbial production, characterization, and applications. *International Journal of Biological Macromolecules, 65*, 454–461.
Larotonda, F. D. S., Torres, M. D., Goncalves, M. P., Sereno, A. M., & Hilliou, L. (2015). Hybrid carrageenan-based formulations for edible film preparation: Benchmarking with kappa carrageenan. *Journal of Applied Polymer Science*, 42263.
Mohammed, S. (2006). Rheological properties of grouts with viscosity modifying agents as diutan gum and welan gum incorporating pulverised fly ash. *Cement and Concrete Research, 36*, 1609–1618.
Nie, G., Zang, Y., Yue, W., Wang, M., Baride, A., Sigdel, A., & Janaswamy, S. (2021). Cellulose-based hydrogel beads: Preparation and characterization. *Carbohydrate Polymer Technologies and Applications, 2*, Article 100074.
Plank, J. (2004). Applications of biopolymers and other biotechnological products in building materials. *Applied Microbiology and Biotechnology, 66*, 1–9.

Plank, J., Lummer, N. R., & Dugonjic-Bilic, F. (2010). Competitive adsorption between an AMPS (R)-based fluid loss polymer and welan gum biopolymer in oil well cement. *Journal of Applied Polymer Science, 116*, 2913–2919.

Polowsky, P. J., & Janaswamy, S. (2015). Hydrocolloid-based nutraceutical delivery systems: Effect of counter-ions on the encapsulation and release. *Food Hydrocolloids, 43*, 658–663.

Rinaudo, M. (2004). Role of substituents on the properties of some polysaccharides. *Biomacromolecules, 5*, 1155–1165.

Rols, S., Ambroise, J., & Péra, J. (1999). Effects of different viscosity agents on the properties of self-leveling concrete. *Cement and Concrete Research, 29*, 261–266.

Sakata, N., Yanai, S., Yoshizaki, M., Phyfferoen, A., & Monty, H. (2001). Evaluation of S-657 biopolymer as a new viscosity-modifying admixture for self-compacting concrete. In K. Ozawa, & M. Ouchi (Eds.), *Proceedings of the 2nd international symposium on self-compacting concrete* (pp. 229–236).

Sandford, P. A., Cottrell, I. W., & Pettitt, D. J. (1984). Microbial polysaccharides: New products and their commercial applications. *Pure Applied Chemistry, 56*, 879–892.

Shannon, R. D. (1976). Revised effective ionic radii and systematic studies of interatomic distances in halides and chalcogenides. *Acta Crystallographica, A, 32*, 751–767.

Sonebi, M. (2006). Rheological properties of grouts with viscosity modifying agents as diutan gum and welan gum incorporating pulverised fly ash. *Cement and Concrete Research, 36*, 1609–1618.

Sonebi, M., & Malinov, S. (2011). Neural network modeling of rheological parameters of grouts containing viscosity-modifying agent. *ACI Materials Journal, 108*, 316–326.

Tako, M., Teruya, T., Tamaki, Y., & Konishi, T. (2009). Molecular origin for rheological characteristics of native gellan gum. *Colloid and Polymer Science, 287*, 1445–1454.

Tenga, L., Meng, W., & Khayata, K. H. (2020). Rheology control of ultra-high-performance concrete made with different fiber contents. *Cement and Concrete Research, 138*, Article 106222.

Wu, C., Li, Y., Du, Y., Wang, L., Tong, C., Hu, Y., Pang, J., & Yan, Z. (2019). Preparation and characterization of konjac glucomannan-based bionanocomposite film for active food packaging. *Food Hydrocolloids, 89*, 682–690.

Yan, J. N., Shang, W. H., Zhao, J., Han, J. R., Jin, W. G., Wang, H. T., Du, Y, N., Wu, H., T., Janaswamy, S., Xiong, Y. L., & Zhu, B. W (2019). Gelation and microstructural properties of protein hydrolysates from trypsin-treated male gonad of scallop (Patinopecten yessoensis) modified by κ-Carrageenan/K^+. *Food Hydrocolloids, 91*, 182–189.

Yu, M., Song, A., Xu, G., Xin, X., Shen, J., Zhang, H., & Song, Z. (2015). 3D welan gum-graphene oxide composite hydrogels with efficient dye adsorption capacity. *RSC Advances, 5*, 75589–75599.